



Direct Evidence of a Characteristic Length Scale of a Dynamical Nature in the Boolchand Phase of Glasses

M. Micoulaut¹ and M. Malki^{2,3}

¹Laboratoire de Physique Théorique de la Matière Condensée, Université Pierre et Marie Curie, CNRS UMR 7600, Boite 121, 4, Place Jussieu, 75252 Paris Cedex 05, France

²CEMHTI, CNRS UPR 3079, 1D, Avenue de la Recherche Scientifique, 45071 Orléans Cedex 02, France

³Université d'Orléans (Polytech'Orléans), BP 6749, 45072 Orléans Cedex 02, France

(Received 23 July 2010; published 3 December 2010)

The ac conductivity spectra of $x\text{AgI}-(1-x)\text{AgPO}_3$ fast-ion conducting glasses spanning the flexible, intermediate (isostatically rigid), and stressed rigid phases are analyzed. The rescaled frequency-dependent spectra are mapped into time-dependent mean-square displacements out of which a typical length scale characterizing the spatial extent $\sqrt{\langle \bar{R}^2(\infty) \rangle}$ of nonrandom subdiffusive regions of ionic motions is computed. The latter quantity is studied as a function of AgI compositions, and is found to display a maximum isostatic compositions, providing the first clear evidence of a typical length scale of a dynamical nature when a system becomes isostatically rigid and enters that phase.

DOI: 10.1103/PhysRevLett.105.235504

PACS numbers: 61.43.Fs

An amorphous network progressively stiffens and becomes rigid as its connectivity or mean coordination number \bar{r} increases. From a mechanical viewpoint, such an evolution can be understood using rigidity theory which considers nearest-neighbor interactions acting at the microscopic level [1], and enumerates the average number of constraints n_c per atom and its balance with respect to the atomic degrees of freedom (3 in three dimensions). This has led to the recognition of a rigidity transition [2,3] separating underconstrained (or flexible, when $n_c < 3$) from overconstrained networks (stressed rigid, when $n_c > 3$). Numerous experiments have confirmed these simple predictions [4], especially in glass science where bulk chalcogenide and oxide glasses have been studied in detail.

While the original theory predicted a single optimized glass composition where the microscopic structure is isostatic (having $n_c \simeq 3$), more recent experiments by Boolchand and coworkers have revealed a second transition [5] for various network-forming glasses, providing a finite width, offering now a whole range of such isostatic compositions, and defining an intermediate phase (IP) bounded by the flexible (at low \bar{r} or n_c) and a stressed, rigid phase (at high \bar{r}). The signature of this phase has been detected in optical, calorimetric, and electrical experiments [6] with clear changes in behavior when the system becomes isostatically rigid for, e.g., complex heat flows at the glass transition or Raman optical elastic power laws. Yet no typical spatial quantity giving rise to a characteristic distance (or length scale) has been observed in the IP, although such an isostatic length scale has been predicted to grow [7] in jammed soft sphere solids which bear some similarities to network glasses. Neutron and high energy x-ray diffraction on chalcogenide glasses have been recently reported [8,9], although a structural origin of the Boolchand IP in typical quantities (e.g., position, width,

and height of the first sharp diffraction peak) related to the static structure factors was not observed.

In this Letter, we show that a length scale associated with the Boolchand intermediate phase appears in the fast ionic conductor $(1-x)\text{AgPO}_3-x\text{AgI}$ in the $9\% < x < 37\%$ AgI range [10]. The present quantity characterizes the spatial extent of subdiffusive ion-motions, and is computed from frequency-dependent conductivity and permittivity data together with linear response theory. The length scale appears to be correlated with calorimetric, optical, or electrical transport quantities that usually reveal the IP, but is neither associated directly with static network structure nor with changes in molar volume, as both evolve smoothly with glass composition. Another length scale characterizing the typical distance mobile ions travel to overcome backward-forward driving forces is found to be only sensitive to the onset of network flexibility at $x = 37\%$ AgI [10]. The present findings highlight, therefore, the clear dynamical nature of the length scale underlying the IP, and underscores a possible connection with the peculiar relaxational phenomena of isostatic glass-forming liquids [11].

Details on the synthesis and the structural, calorimetric, electrical, and spectroscopic properties of dry and homogeneous bulk $(1-x)\text{AgPO}_3-x\text{AgI}$ glasses were discussed earlier in Refs. [12,13]. The complex impedance $Z^*(\omega) = Z'(\omega) + iZ''(\omega)$ was measured by a Solartron SI 1260 impedance analyzer over the frequency range of 1 Hz–1 MHz. Three temperatures have been considered: 250, 300, and 350 K. Conductivity $\sigma^*(\omega)$ was deduced from the complex impedance $Z^*(\omega)$. The real part of the dielectric permittivity $\epsilon'(\omega)$ was computed using the electrical modulus M^* : $M^* = 1/\epsilon^* = i\omega\epsilon_0/\sigma^*$, where ϵ_0 is the permittivity of free space.

Figure 1(a) shows the log-log plot of the real part of the conductivity with frequency at three different temperatures

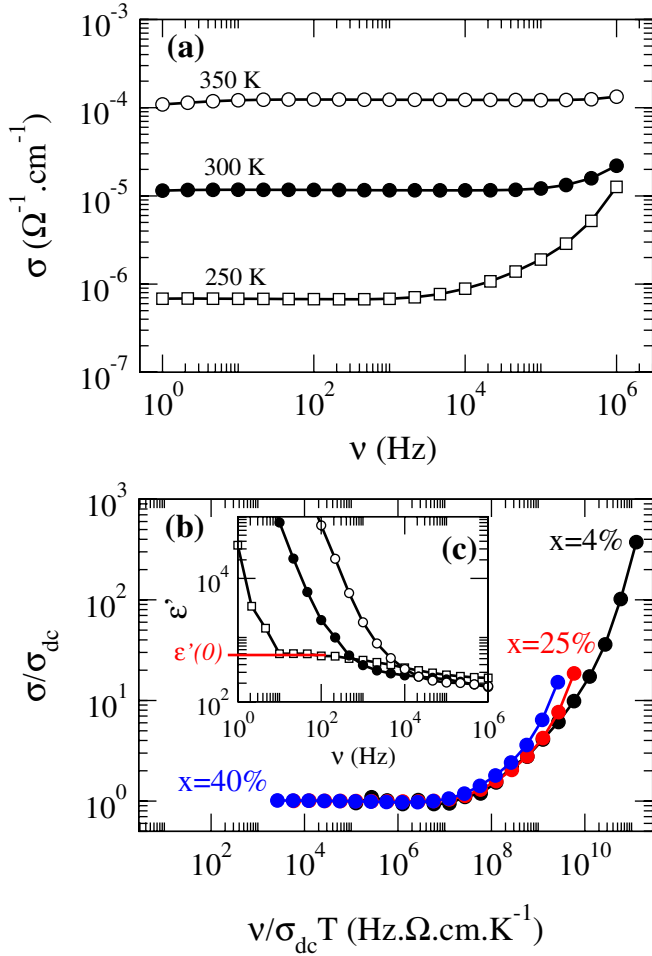


FIG. 1 (color online). (a) Experimental conductivities of a 25AgI-75AgPO₃ glass at three different temperatures and corresponding (c) dielectric permittivities. The (red) horizontal line serves to define the low-frequency permittivity $\epsilon'(0)$ used in Eq. (2). (b) Master curve $\sigma/\sigma_{\text{dc}}$ as a function of the rescaled frequency $\nu/\sigma_{\text{dc}}T$ for three selected compositions at $T = 250$ K, derived from the experimental conductivities.

for a glass at $x = 25\%$ AgI. Dielectric permittivity spectra $\epsilon'(\omega)$ were computed [Fig. 1(c)] and tracked with composition [6]. Concerning the latter, the electrode polarization effect onsets at low frequency manifested by a rapid growth of ϵ' . This phenomenon hides the intrinsic frequency behavior of $\epsilon'(\omega)$ so that an evaluation of the limit $\epsilon'(0)$ [defined in Fig. 1(c)] is only possible at low temperature. At low frequency and low temperature (250 K), we obtain a dc régime which displays an Arrhenius behavior, whereas at higher frequencies a dispersive régime is observed, with σ or ϵ' becoming frequency dependent. A frequency $\nu_p(x, T)$ satisfying $\sigma(\nu_p)/\sigma_{\text{dc}} = 2$ is usually introduced to characterize the crossover range between the dc and dispersive conductivity régimes, the latter being associated with a subdiffusive régime in the time domain valid for $t < t_p = 1/(2\pi\nu_p)$. The frequency ν_p increases with increasing temperature, and a simple rescaling by a factor $\sigma_{\text{dc}}T$ has been proposed [14] in order to produce a

master curve for various temperatures and compositions. Results are shown in Fig. 1(b) for three selected compositions which show indeed that the data nearly map onto the same curve.

We now build on the linear response theory developed by Roling and coworkers [15,16] and recently applied to borophosphate glasses [17]. It allows extracting from conductivity spectra a mean-square displacement $\langle r^2(t) \rangle$ of the mobile ions given by

$$\begin{aligned} \langle r^2(t) \rangle &= \frac{12k_B T H_R}{N_v q^2 \pi} \int_0^t dt' \int_0^\infty \frac{\sigma(\nu)}{\nu} \sin(2\pi\nu t') d\nu \\ &= \langle R^2(t) \rangle H_R. \end{aligned} \quad (1)$$

N_v is the charge density, and $\langle R^2(t) \rangle$ is the mean-square displacement of the center of charge of the mobile ions. H_R is the so-called Haven ratio [16], found usually between 0.2 and 1.0 and depends on the concentration of charge carriers [18,19]. It characterizes the degree of cooperativity of ion motion and can only be obtained by combining measurement of σ_{dc} with the low-frequency limit of the self-diffusion constant $D'(0)$. As H_R is not known for the present system, we focus on $\langle R^2(t) \rangle$. From the permittivity spectra, one can extract [15,16] the long-time limit of a rescaled quantity, $\langle \tilde{R}^2(\infty) \rangle$, using $\langle R^2(t) \rangle$, given by

$$\begin{aligned} \langle \tilde{R}^2(\infty) \rangle &= \lim_{t \rightarrow \infty} [\langle R^2(t) \rangle - 6D'(0)t] \\ &= \frac{6k_B T \epsilon_0}{N_v q^2} [\epsilon'(0) - \epsilon'(\infty)] \end{aligned} \quad (2)$$

Figure 2 shows $\langle R^2(t) \rangle$ for three selected compositions corresponding to the flexible (40% AgI), intermediate (25%), and stressed rigid phase (4%), computed from Eq. (1). At long time ($t > t_p$), $\langle R^2(t) \rangle$ displays the diffusive régime as detected from the slope of 1 in the log-log plot, while a subdiffusive régime corresponding to correlated forward-backward motions appears at shorter times scales ($t < t_p$). Here the limit t_p (or its rescaled quantity $t_p \sigma_{\text{dc}} T$) designates the time beyond which ions start to diffuse. One can therefore consider the characteristic length $\sqrt{\langle R^2(t_p) \rangle}$ to be the typical distance mobile ions have to travel to overcome the interactions responsible for these forward-backward motions [see Fig. 2 inset]. The quantity $\langle \tilde{R}^2(\infty) \rangle$ given by Eq. (2) provides a measure of the spatial extent [Fig. 2, inset] of subdiffusive motions (SDR) [16], made of back and forth hops between local traps. Molecular dynamics simulations provide an accurate atomic scale picture of these SDR. In Ag chalcogenides [20] the ion dynamics is indeed made of localized motions between local trapping centers giving rise to subdiffusive motion. These trapping centers are separated by a distance corresponding to $\sqrt{\langle R^2(t_p) \rangle}$. Similar results are found in sodium silicates [21], which show that subdiffusive pockets have

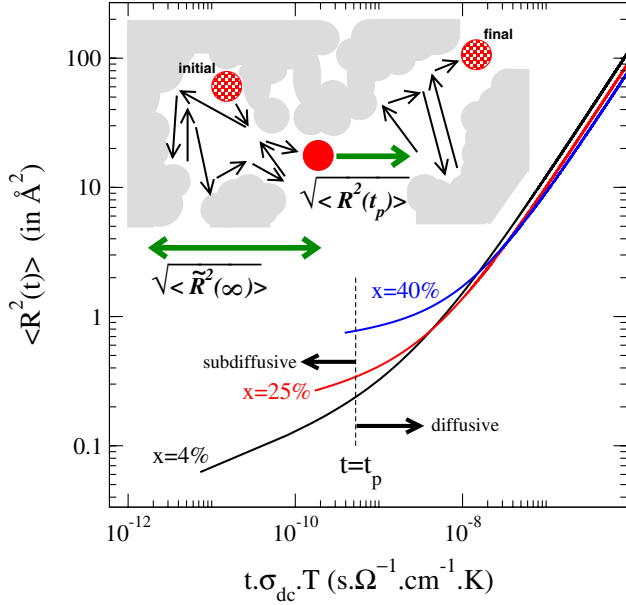


FIG. 2 (color online). Mean-square displacement $\langle R^2(t) \rangle$ at 250 K of $(1-x)\text{AgPO}_3-x\text{AgI}$ at three selected compositions representing the three phases of interest, derived from the master curve represented in Fig. 1 and Eq. (1) as a function of rescaled time $t\sigma_{dc}T$. The vertical broken line corresponds to the abscissa $t_p\sigma_{dc}T$, defining t_p for a glass at $x = 4\%$, the approximate limit between the diffusive and subdiffusive régimes. Inset: Trajectory of an ion between an initial and a final state, which serves to define the quantities $\sqrt{\langle \bar{R}^2(\infty) \rangle}$ and $\sqrt{\langle R^2(t_p) \rangle}$.

a spatial extent of about 6–7 Å (for the largest), and are separated by a distance which is smaller (2 Å).

Both length scales $\sqrt{\langle R^2(t_p) \rangle}$ and $\sqrt{\langle \bar{R}^2(\infty) \rangle}$ can be determined from the conductivity and permittivity spectra, and we follow these with AgI content of glasses. Results are displayed in Fig. 3. $\sqrt{\langle \bar{R}^2(\infty) \rangle}$ displays a maximum in the Boolchand intermediate phase, driven mainly by a maximum in the permittivity difference $\varepsilon'(0) - \varepsilon'(\infty)$ appearing in Eq. (2) [6]. Starting from 5.5 Å at $x = 0$, this length scale increases up to a maximum of nearly 9 Å in the IP and then decreases to 2.5 Å in the flexible phase. In the present system, $\sqrt{\langle \bar{R}^2(\infty) \rangle}$ is found to be larger than $\sqrt{\langle R^2(t_p) \rangle}$, the latter being of the order of 0.5–1.5 Å, which is similar to what has been found in borophosphate glasses [17]. The same situation is met in sodium borates [16] but differs in sodium germanates where $\sqrt{\langle R^2(t_p) \rangle}$ is found to be of the same order (8 Å) as the spatial extent. These collected results suggest that both $\sqrt{\langle R^2(t_p) \rangle}$ and $\sqrt{\langle \bar{R}^2(\infty) \rangle}$ are strongly structure, composition, and system dependent. One should also keep in mind that in contrast with the latter, the present network former already contains here the diffusing Ag ion.

Trends in $\sqrt{\langle \bar{R}^2(\infty) \rangle}$ as a function of x correlate with those in the nonreversing heat flow, ΔH_{nr} , obtained from

calorimetric measurements [10], and with the three régimes for dc conductivity [Fig. 3(b)]. These trends cannot be explained on the basis of free volume changes induced by AgI doping as molar volumes are known [13] to decrease linearly. The global maximum of $\sqrt{\langle \bar{R}^2(\infty) \rangle}$ found at around $x = 20\%$ shows that in the “stress-free” Boolchand intermediate phase, ion dynamics are quite different from those in the elastic phases (flexible, stressed) formed above and below. These results suggest that there is a maximum in spatial extent of subdiffusive motions in the IP. At low AgI concentrations, isolated SDR are embedded in a stressed rigid structure and lead to a low spatial extent. The increase of the number of hopping sites in the IP [6] leads to a growth of the subdiffusive regions (and $\sqrt{\langle \bar{R}^2(\infty) \rangle}$). Finally, the spatial extent of these regions decreases at higher x . Reverse Monte Carlo simulations shows that for this system the Ag pathways are localized in small conduction “trees” at low AgI concentration [22] which percolate in the region $0.2 < x < 0.3$ to a single pathway. As a result, the spatial extent of localized motions must decrease. Figure 3 illustrates for the first time that a typical length scale is associated with the IP, which is of dynamical origin as it is computed from the mean-square

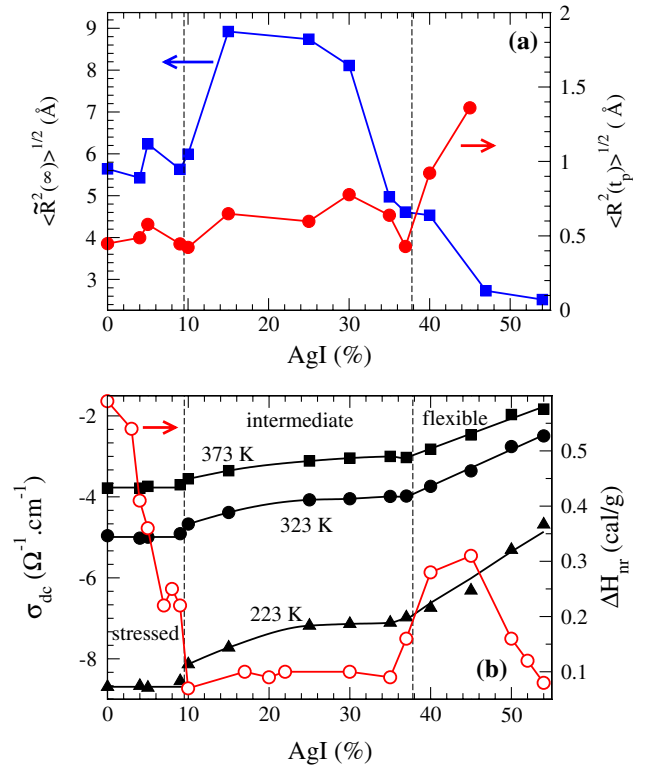


FIG. 3 (color online). (a) Plot of the characteristic length scales $\sqrt{\langle \bar{R}^2(\infty) \rangle}$ (blue) and $\sqrt{\langle R^2(t_p) \rangle}$ (red, right axis) in $(1-x)\text{AgPO}_3-x\text{AgI}$ as a function of AgI composition, compared to (b) (extracted from Ref. [6]): conductivity σ_{dc} (black filled symbols) at different temperatures and nonreversing heat flow ΔH_{nr} [open (red) circles, right axis]. The vertical broken lines define the intermediate phase boundaries.

displacement. There is no structural origin of such a length scale because relevant quantities deduced from x-ray diffraction [23] behave smoothly with composition, an observation also reported on a different system in [9].

The other quantity of interest, the length scale $\sqrt{\langle R^2(t_p) \rangle}$, is found to display a threshold at the intermediate to flexible transition [Fig. 3, right axis], also known as the rigidity transition. In fact, as long as the system is rigid (stressed or isostatic), this length scale remains nearly constant at about 0.5 Å, largely because a large energy is needed to locally deform the network in order to overcome the backward driving forces causing the correlated subdiffusive forward-backward motions. One control parameter of $\sqrt{\langle R^2(t_p) \rangle}$, the time t_p for the onset of diffusion decreases from 400 μs at $x = 0$ to 10–15 μs close to the flexible transition (37%–40%). Once the system has become flexible and floppy modes proliferate, ion motion is facilitated and the time decreases to $t_p = 6.7 \mu\text{s}$ at $x = 45\%$ AgI. At this concentration, and because of the large number of carriers, the time needed to leave a SDR reduces, but a larger distance is needed to overcome the backward driving forces induced by the presence of an increased number of Ag cations.

In summary, we have shown for the first time that a typical length scale, of a dynamical origin, is associated with the Boolchand Intermediate Phase. This length scale appears in fast-ion conducting glasses, and measures the spatial extent of subdiffusive ionic motions that increase when the system becomes isostatic and decreases once conduction pathways percolate in the flexible phase. Another length scale characterizing the forward-backward motion at play in the subdiffusive régime is found to signal only the intermediate to flexible transition. Length scales associated with dynamical heterogeneities are also found in the glass transition region [24]. While focused on the glassy state, the present study can not be extended to higher temperatures because electrode polarization at higher T will lead to the impossibility of measuring the saturating $\epsilon''(0)$, and thus the behavior of $\sqrt{\langle \tilde{R}^2(\infty) \rangle}$ with T . However, from our results found at 250 K and from the reported observations [25] of the IP at the glass transition, we can sketch a certain number of salient features which correlate with the obtained compositional dependence of the characteristic length scale. IP glass-forming liquids have a high configurational entropy and display weak kinetic changes ($\Delta H_{\text{nr}} = 0$) and low aging phenomena once $T < T_g$ [25], which are associated with maximized length scale for the Ag mobile ions in the present system. Does this length scale exist also for the much slower network diffusing ions (P,O) ? This question remains open at this stage but it is known that anomalies have been observed in network glass-forming liquids such as binary Ge-Se [11,26] for the IP compositions.

It is a pleasure to acknowledge many stimulating discussions with M. Bauchy, P. Boolchand, B. Goodman,

J.C. Mauro, J. C. Phillips, B. Roling, and P. Simon. This work is supported by Agence Nationale de la Recherche (ANR) No. 09-BLAN-0190-01.

-
- [1] *Rigidity Theory and Applications*, edited by M. F. Thorpe and P. M. Duxbury (Kluwer Academic, Plenum Publishers New York, 1999).
 - [2] J. C. Phillips, *J. Non-Cryst. Solids* **34**, 153 (1979).
 - [3] M. F. Thorpe, *J. Non-Cryst. Solids* **57**, 355 (1983).
 - [4] *Rigidity and Boolchand Intermediate Phases in Nanomaterials*, edited by M. Micoulaut and M. Popescu (INOE Publishing House, Bucharest, 2009).
 - [5] D. Selvanathan, W. J. Bresser, P. Boolchand, and B. Goodmann, *Solid State Commun.* **111**, 619 (1999).
 - [6] M. Micoulaut, M. Malki, D. I. Novita, and P. Boolchand, *Phys. Rev. B* **80**, 184205 (2009).
 - [7] M. Wyart, *Ann. Phys. (Paris)* **30**, 1 (2005).
 - [8] E. Bychkov, C. J. Benmore, and D. L. Price, *Phys. Rev. B* **72**, 172107 (2005).
 - [9] M. T. M. Shatnawi, C. L. Farrow, Ping Chen, P. Boolchand, A. Sartbaeva, M. F. Thorpe, and S. J. L. Billinge, *Phys. Rev. B* **77**, 094134 (2008).
 - [10] D. I. Novita, P. Boolchand, M. Malki, and M. Micoulaut, *Phys. Rev. Lett.* **98**, 195501 (2007).
 - [11] M. Micoulaut, *J. Phys. Condens. Matter* **22**, 285101 (2010).
 - [12] D. I. Novita and P. Boolchand, *Phys. Rev. B* **76**, 184205 (2007).
 - [13] D. I. Novita, P. Boolchand, M. Malki, and M. Micoulaut, *J. Phys. Condens. Matter* **21**, 205106 (2009).
 - [14] B. Roling, A. Happe, K. Funke, and M. D. Ingram, *Phys. Rev. Lett.* **78**, 2160 (1997).
 - [15] B. Roling, C. Martiny, and K. Funke, *J. Non-Cryst. Solids* **249**, 201 (1999).
 - [16] B. Roling, C. Martiny, and S. Bruckner, *Phys. Rev. B* **63**, 214203 (2001).
 - [17] D. Zielniok, H. Eckert, and C. Cramer, *Phys. Rev. Lett.* **100**, 035901 (2008).
 - [18] D. L. Sidebottom, P. F. Green, and R. K. Brow, *J. Non-Cryst. Solids* **222**, 354 (1997).
 - [19] G. N. Greaves and K. L. Ngai, *Phys. Rev. B* **52**, 6358 (1995).
 - [20] I. Chaudhuri, F. Inam, and D. A. Drabold, *Phys. Rev. B* **79**, 100201 (2009).
 - [21] P. Jund, W. Kob, and R. Jullien, *Phys. Rev. B* **64**, 134303 (2001).
 - [22] J. D. Wicks, L. Börjesson, G. Bushnell-Wye, W. S. Howells, and R. L. McGreevy, *Phys. Rev. Lett.* **74**, 726 (1995).
 - [23] H. Takakashi, E. Matsubara, and Y. Waseda, *J. Mater. Sci.* **29**, 2536 (1994).
 - [24] A. Coniglio, T. Abete, A. de Candia, E. Del Gado, A. Fierro, *J. Phys. Condens. Matter* **20**, 494239 (2008).
 - [25] P. Boolchand, M. Micoulaut, and P. Chen in *Nature of Glasses, in Phase Change Materials: Science and Applications*, edited by S. Raoux and M. Wuttig (Springer, Heidelberg, 2008).
 - [26] S. Stolen, T. Grande, and H.-B. Johnsen, *Phys. Chem. Chem. Phys.* **4**, 3396 (2002).